Improving Analysis of Low Voltage Ride Through Capability in Turbines Connected to The Brushless Doubly Fed Induction Generator (BDFIG) under Fault Conditions

Maryam Alizadeh, Reza ghazi, Ehsan Erfani Haghani
Department of Electrical Engineering
Ferdowsi University of Mashhad
Mashhad, Iran
Maryam.alizadeh1990@yahoo.com rghazi@um.ac.ir
ehsanerfanih@yahoo.com

Mohammad Esmaeili Rad
Department of Electrical Engineering
Hakim sabzevari university
Sabzevar, Iran
Mohammad.es5153@gmail.com

***Abstract*— The connection of wind farms to the grid and their dynamic behavior under different conditions is a real challenging issue which resulted in providing new instructions for the network. One of the important topics related to grid standards is Low-Voltage Ride-Through capability. In recent years, The application of Brushless Doubly Fed Induction Generator (BDFIG) in the wind farms has drawn the attention of researchers.. This generator has more advantages than other common generators, including the Doubly Fed Induction Generator (DFIG). In this paper, the performance of the BDFIG under fault conditions in the grid is examined and monitored in order to improve LVRT while considering the dynamic model of the BDFIG connected to a wind turbine. In this method, the reactive power and speed are controlled for stable performance of the generator under various grid conditions. A converter is used to connect the stator control winding to the power grid, which DC link voltage is adjusted using multiple PI controllers under fault conditions. In addition, two controlling systems based on the conventional PI controllers are proposed to control the generator side converter and the wind turbines step angle. The results demonstrate good dynamic performance of the examined generator under different grid conditions achieved by the proposed controlling method without using any additional hardware such as a Crowbar.**

Keywords*— *Low-Voltage Ride-Through (LVRT) Capability, Wind farms, Renewable energies, Brushless Doubly Fed Induction Generator (BDFIG), Fault Ride-Through (FRT)

I. INTRODUCTION

The Low-Voltage Ride-Through (LVRT) capability or Fault Ride-Through (FRT) capability in the wind turbines means that the generator connected to the wind turbines must stands the voltage drop in their terminals and remain connected to the grid during and after the fault. The voltage drop may occur as a result of a short circuit, start-up of induction machines, disconnection of capacitors, etc. In power systems where wind turbine power covers a large portion of the network power, in the case of disconnecting wind turbines from the grid, it will experience electricity cut-off and power shortages. As the scale of wind farms grows, the conditions and procedures which connect the wind turbines to network become more important. Therefore, a power generation capability is also required for anomalous grid conditions and compliance with the LVRT requirements in accordance with the grid standards. There are different structures for wind turbines depending on the generator type, power electronics converter, generator speed change range, and the mechanical connection of the generator rotor. Some generators are more suitable for use in the wind power plants due to the periodic and intermittent feature of wind. Because of the more advantages of BDFIG in comparison to other generators in the case of LVRT operation, this generator has drawn the attention of numerous researchers in recent years [1]. A controlling method for BDFIG in wind turbines to tolerate symmetrical faults is using of hysteresis comparator based on detecting voltage drop, and controller operating at LVRT when the symmetrical faults is diagnosed by detector will operate. When a fault occurs only positive sequence will be controlled by controller, and neutral and negative sequence will cause transient response and unbalances, respectively which needs using of a filter and result in a complicated controlling system that covers symmetrical voltage drops only [2]. In another method dynamic behavior of BDFIG at three phase symmetrical voltage drops is proposed. In this model full and partial voltage drops is evaluated using vector methods. As a result of grid faults, significant voltages will appear at control windings terminal. Stable and transient behavior of voltages illustrates that induced voltage at DC link increased especially in the case of operation at more than natural speed which result in inducing considerable inrush current at control windings. Hence, system needs DC link of inverter having more capacity [3]. Using of such hardware equipment as crowbar and series dynamic resistance, is a suggestion for tolerating low voltages when fault occurs which is more expensive in comparison to software methods [4], [5]. In this article, after introducing dynamic behavior of the machine, a controlling system based on typical PI controllers will be proposed, then simulation results in correspondence with network standards will be illustrated.

978-1-7281-5273-8/19/$31.00 ©2019 IEEE

II. BDFIG MODELING

A. Dynamic performance

The BDFIG stator has two windings that are different in the number of pairs of poles to avoid the direct connection between the windings. The rotor is specifically designed to connect the two stator windings [6]. Generally, the 1-stator winding is directly connected to the grid power, and thus, it is known as the power winding (PW). In contrast, the 2-stator winding, called the control winding (CW), is supplied with a voltage-varying frequency converter and manages only a small part of the effective power. The BDFIG can operate in various modes, including the synchronous (dual fed) mode, cascade mode, and the induction mode [7]. The synchronous mode is the most optimal model where the shaft speed is independent of the torque applied to the device and can be formulated as follows:

$$w_r = \frac{w_1 + w_2}{p_1 + p_2} \tag{1}$$

Where w_1 and w_2 are the angular frequency of excitation with two stator windings. When w_2 is zero, the rotor rotates at the normal speed.

B. Mathematical presentation of vector modeling

For simplicity, the controller provided is synchronized with the PW flux frame. Thus:

$$\psi_{1d} = |\psi_1| \tag{2}$$

$$\psi_{1q} = 0 \tag{3}$$

The model at the PW flux frame is as follows [8] [9]:

$$v_1 = R_{S1} i_1 + \frac{d\psi_1}{dt} + j w_1 \psi_1 \tag{4}$$

$$\psi_1 = L_{s1} i_1 + L_{s1r} i_r \tag{5}$$

$$v_2 = R_{s2} i_2 + \frac{d\psi_2}{dt} + j\left(w_1 - (p_1 + p_2) w_r\right)\psi_2 \tag{6}$$

$$\psi_2 = L_{s2} i_2 + L_{s2r} i_r \tag{7}$$

$$v_r = R_r i_r + \frac{d\psi_r}{dt} + j\left(w_1 - p_1 w_r\right)\psi_r \tag{8}$$

$$\psi_r = L_r i_r + L_{s1r} i_{1+} L_{s2r} i_2 \tag{9}$$

The electric torque is also as follows:

$$T_e = \frac{3}{2} p_1 \operatorname{Im}\left[\psi_1^* i_1\right] + \frac{3}{2} p_2 \operatorname{Im}\left[\psi_2 i_2^*\right] \tag{10}$$

Since the voltages and currents are respectively the input and output in the dynamic modeling of this type of machine, entering the voltage values result in calculating the currents. The equations can be written in terms of flux using formulas 5, 7, and 9. Since we incorporate the equations in the dq two-axis frame, then, we have:

$$\psi_{1d} = L_{s1} i_{1d} + L_{s1r} i_{rd} \tag{11}$$

$$\psi_{1q} = L_{s1} i_{1q} + L_{s1r} i_{rq} \tag{12}$$

$$\psi_{2d} = L_{s2} i_{2d} + L_{s2r} i_{rd} \tag{13}$$

$$\psi_{2q} = L_{s2} i_{2q} + L_{s2r} i_{rq} \tag{14}$$

$$\psi_{rd} = L_r i_{rd} + L_{s1r} i_{1d} + L_{s2r} i_{2d} \tag{15}$$

$$\psi_{rq} = L_r i_{rq} + L_{s1r} i_{1q} + L_{s2r} i_{2q} \tag{16}$$

$$v_{1d} = R_{S1} i_{1d} + \frac{d\psi_{1d}}{dt} - w_1 \psi_{1q} \tag{17}$$

$$v_{1q} = R_{S1} i_{1q} + \frac{d\psi_{1q}}{dt} + w_1 \psi_{1d} \tag{18}$$

$$v_{2d} = R_{S2} i_{2d} + \frac{d\psi_{2d}}{dt} - \left(w_1 - (p_1 + p_2) w_r\right)\psi_{2q} \tag{19}$$

$$v_{2q} = R_{S2} i_{2q} + \frac{d\psi_{2q}}{dt} + \left(w_1 - (p_1 + p_2) w_r\right)\psi_{2d} \tag{20}$$

$$v_{rd} = R_r i_{rd} + \frac{d\psi_{rd}}{dt} - \left(w_1 - p_1 w_r\right)\psi_{rq} \tag{21}$$

$$v_{rq} = R_r i_{rq} + \frac{d\psi_{rq}}{dt} + \left(w_1 - p_1 w_r\right)\psi_{rd} \tag{22}$$

By combining the equations of voltage and flux, we can obtain the current relations based on flux in the dq two-axis frame:

$$i_{1d} = \frac{\psi_{1d} L_{s2r}^2 - L_{s1r} L_{s2r} \psi_{2d} - L_r L_{s2} \psi_{1d} + L_{s2} L_{s1r} \psi_{rd}}{L_{s2} L_{s1r}^2 + L_{s1} L_{s2r}^2 - L_r L_{s1} L_{s2}} \tag{23}$$

$$i_{1q} = \frac{\psi_{1q} L_{s2r}^2 - L_{s1r} L_{s2r} \psi_{2q} - L_r L_{s2} \psi_{1q} + L_{s2} L_{s1r} \psi_{rq}}{L_{s2} L_{s1r}^2 + L_{s1} L_{s2r}^2 - L_r L_{s1} L_{s2}} \tag{24}$$

$$i_{2d} = \frac{\psi_{2d} L_{s1r}^2 - L_{s1r} L_{s2r} \psi_{1d} - L_r L_{s1} \psi_{2d} + L_{s1} L_{s2r} \psi_{rd}}{L_{s2} L_{s1r}^2 + L_{s1} L_{s2r}^2 - L_r L_{s1} L_{s2}} \tag{25}$$

$$i_{2q} = \frac{\psi_{2q} L_{s1r}^2 - L_{s1r} L_{s2r} \psi_{1q} - L_r L_{s1} \psi_{2q} + L_{s1} L_{s2r} \psi_{rq}}{L_{s2} L_{s1r}^2 + L_{s1} L_{s2r}^2 - L_r L_{s1} L_{s2}} \quad (26)$$

$$i_{rd} = \frac{L_{s2} L_{s1r} \psi_{1d} - L_{s1} L_{s2} \psi_{rd} + L_{s1} L_{s2r} \psi_{2d}}{L_{s2} L_{s1r}^2 + L_{s1} L_{s2r}^2 - L_r L_{s1} L_{s2}} \quad (27)$$

$$i_{rq} = \frac{L_{s2} L_{s1r} \psi_{1q} - L_{s1} L_{s2} \psi_{rq} + L_{s1} L_{s2r} \psi_{2q}}{L_{s2} L_{s1r}^2 + L_{s1} L_{s2r}^2 - L_r L_{s1} L_{s2}} \quad (28)$$

Also, the electrical torque in the dq two-axis frame is calculated as follows:

$$T_e = \frac{3}{2} p_1 \left[\psi_{1d} i_{1q} - \psi_{1q} i_{1d} \right] + \frac{3}{2} p_2 \left[\psi_{2q} i_{2d} - \psi_{2d} i_{2q} \right] \quad (29)$$

As shown in Figure 1, the power winding is directly connected to the power grid and has the grid frequency. Thus we will have.

$$w_1 = 50 \times 2\pi = 100\pi, f = 50Hz \quad (30)$$

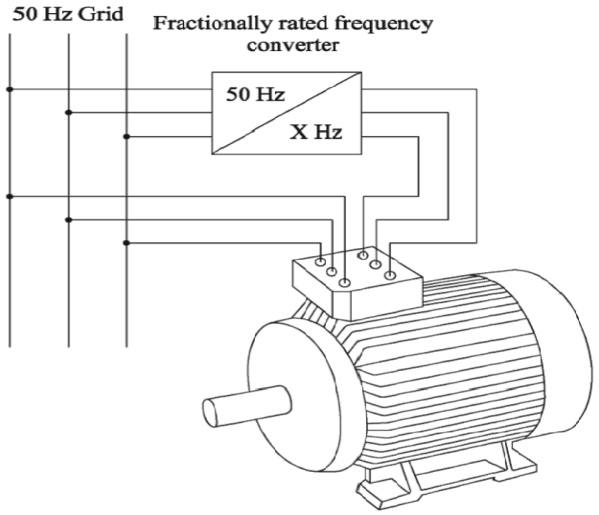

Fig. 1. Schematic of BDFIG.

Therefore, the power winding has a constant angular speed.

III. BDFIG BEHAVIOR UNDER GRID LOW-VOLTAGE

The Park model is commonly used to analyze induction generators. The induced electromotive force is the derivative of the stator control winding leakage flux. In the case of grid faults, due to the symmetrical component theory [10], the stator voltage can be divided into three parts: Positive sequence, negative sequence, and zero sequence.

The BDFIG is usually installed at high voltage by Δ-Y transformators to increase its voltage since the star side is connected to the high voltage and it is possible to ground the neutral point. Therefore, the neutral component does not exist in the stator terminals and can be ignored. The induced EMF during the grid voltage drop is expressed as the following relation:

$$E = \frac{1}{2} k_{sr} v_p e^{jw_1 t} + k_{sr} v_n e^{-jw_1 t} - C_1 v_n t e^{-jw_1 t} + C_2 e^{-jw_1 t} \quad (31)$$

Where C is the coefficient resulted from simplification. As can be seen in relation (31), the EMF is the sum of 4 parts: The negative flux component rotates at speed -w1 and consists of two parts. There are also the positive component and the transient component. Therefore, the total EMF under asymmetrical voltage drop is also higher than the normal conditions, and subsequently, the induced EMF may exceed the converter's maximum voltage of the stator control wingding side at higher voltage drops of the grid and create out-of-control currents.

The DC link voltage also increases at the same time and large inrush currents appear in the stator control winding circuit. If these currents exceed the limit that the converter can tolerate, significant damage may occur. In addition, under an asymmetrical drop, if the crowbar is used to protect the converter in the considered BDFIG, it should operate during all time of the voltage drop, especially in the case of deeper drops that cause the generator to absorb a large amount of reactive power from the grid and worsen the grid voltage drop. In these cases, the grid requirements cannot support the recovery of the grid voltage.

IV. PROPOSED CONTROL METHOD

A. Control System of Grid Side Converter

In this section, a DC link voltage regulator system is used based on the BDFIG stator power winding current regulation to control the DC link voltage in the average model converter provided on the grid side. Figure 2 shows a schematic of this control system. As can be seen in the Figure, three PI controllers are used to control the DC link voltage in the average model converter, to keep this voltage to a value close to the reference value of 1100 (v).

This control system is based on controllers operating in the dq synchronous rotary frame. The controller gives the i_{1d} voltage as a reference to the average model converter on the inverter side. The current control loops are responsible for controlling the average model converter during the grid normal operation. The reference DC link voltage can be adjusted based on the proposed controllers depending on the grid operating conditions in the case of fault and the grid power and load values.

We obtained three-phase voltage values for the parameters used in the two d and q reference frames by controlling the voltages of the grid converter side and converting the dq two-axis frame and used these values in the average model converter to get the value of the controlled DC link voltage. To better control the DC link voltage when a fault occurs, this voltage was passed through a low-pass filter.

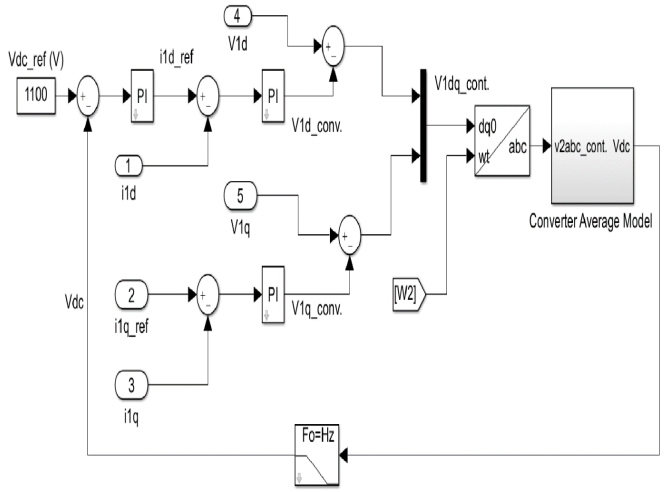

Fig. 2. Schematic of control system of DC link voltage.

B. Control System of Stator Control Winding Side Converter

The In the proposed system, the active and reactive powers are delivered to the grid based on the studied control model, which is designed to provide a satisfactory dynamic performance in the real operation space under fault conditions and voltage drop in the grid with high similarity between the simulated model and the real model, which has control functions: 1)Wind-based reactive power simulator, 2)Open-loop control using logical commands, 3)Electric control system. The overall block diagram of the control system model is shown in Fig. 3.

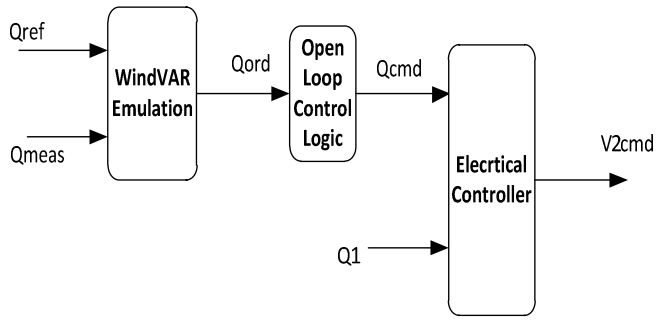

Fig. 3. Schematic of control system of CW side converter.

1) Wind-based Reactive Power Simulator

Terms of this function provide a simple system containing VAR controllers for wind farms. This function monitors the voltage of a specified bus, which compensates for the drop in the line and compares it with the reference voltage. The regulator itself is a PI controller with a Tv time constant. This time constant represents a delay that depends on the type of generator used and is needed to maintain stability. The measurement delay is shown by the time constant Tr. Figure 4 illustrates the schematic diagram of this control system. Qmeas and Vmeas represent the reactive power generated by the wind turbine and the grid-side converter voltage.

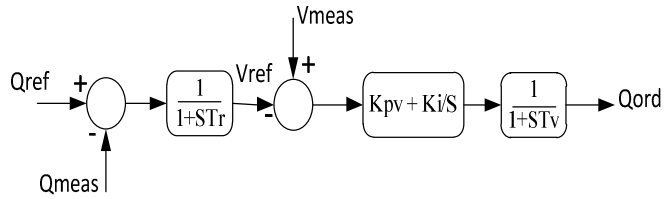

Fig. 4. Schematic of Wind-based reactive power simulator.

2) Open-loop Control Using Logical Commands

This control system corresponds to large changes in the system voltage and is off (inactive) whenever the converter terminal voltage on the generator side is within its normal range. The performance process of the control model is described in Table 1. The functions in this table show the type of open-loop controls applied to improve the system performance when the fault occurs in the grid. Hysteresis is also needed to prevent possible damages like all open-loop controllers of this type. When the voltage thresholds pass and the reactive power loop command is issued, the threshold voltage changes with a certain V_{hyst} value.

TABLE I. PARAMETERS OF OPEN-LOOP CONTROL SYSTEM

Voltage conditions	Period	Open-loop reactive power command
Vterm < V_{L1}	t < T_{L1}	Q_{L1}
	T_{L1} < t < T_{L2}	Q_{L2}
	t > T_{L2}	Q_{L3}
Vterm > V_{H1}	t < T_{H1}	Q_{H1}
	T_{H1}< t < T_{H2}	Q_{H2}
	t > T_{H2}	Q_{H3}

3) Electric Control System

This controller calculates and controls the reactive power of the generator and the terminal voltage of the generator-side converter with voltage commands. In the proposed control system, the terminal voltage is compared with the reference voltage to determine the error voltage (Verr) value. Then this error is increased by a "Gain" and coordinated with the voltage commands. The value of this “Gain” determines the effective time constant proportional to the voltage control loop. The voltage command value is limited. Figure 5 illustrates the schematic diagram of this control system.

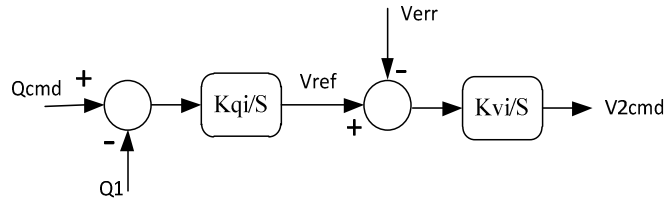

Fig. 5. Schematic of Electric control system.

C. Wind Turbine Control Model

This model provides a simple representation of a complex electromechanical system. The function of the wind turbine is to extract power from wind and the wind turbine model includes the algebraic relations governing the mechanical power of the shaft, wind speed, and the step. The applied concept of wind turbine control describes that when the available wind power exceeds the effective amount of equipment, the blades are adjusted to reduce axial the mechanical power (Pmech) delivered to the shaft. When the available wind power is less than the effective value, the blades are adjusted to their minimum step for maximum mechanical power [10]. In each of these cases, the turbine control system measures the shaft speed and tries to get the device back to its nominal speed. The turbine control model sends the requested power to the electrical control system, which is proportional to the power demanded by the converter that powers the grid. The electrical power, which is actually transmitted to the grid, goes back to the turbine model. For power levels below the effective value, the turbine speed is mainly controlled by the electrical power proportional to the specified reference speed value. For power levels above the effective value, the rotor speed is mainly controlled by controlling the step. The reference speed is usually 1.2 pu. In general, the reference speed value is calculated from the following equation.

$$w_{ref} = -0.67P_1^2 + 1.42P_1 + 0.51 \quad (32)$$

The speed reference slowly follows the power changes with a time constant of about 5 seconds. The turbine control acts as such to counteract fluctuations in the electrical power to be proportional to changes in the axle power. The wind turbine control model is shown in Figure 6.

V. Simulation Results

The simulation results have been presented for the proposed control model in two separate subdivisions. To prove the correct performance of the machine during grid faults, we simulated the proposed control system both in symmetrical and in asymmetrical drop modes.

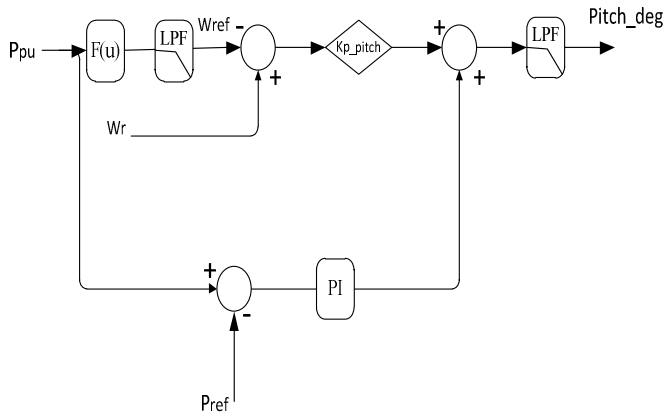

Fig. 6. Schematic of Wind turbine control model.

A. Performance of The Proposed Structure During Three-Phase Symmetrical Voltage Drop

When a three-phase symmetrical fault occurs in the grid with a 100% voltage drop, at the first moment of the drop occurrence, the currents of control and power windings of the stator exceed 2 pu that the current values of both stator windings will reach a controllable value with the function of the mentioned controllers during the fault occurrence. In the proposed structure, the occurrence of the fault is applied at moments between 3.5 and 3.7 seconds.

As shown in Figures 7 and 8, the drop value in the control winding is lower than the power winding. Figures 9 and 10 shows the amount of stator power and control winding currents during the fault conditions in the grid. By comparing the current between the BDFIG stator control and power windings, as seen, both currents are well controlled after a short time of the fault occurrence.

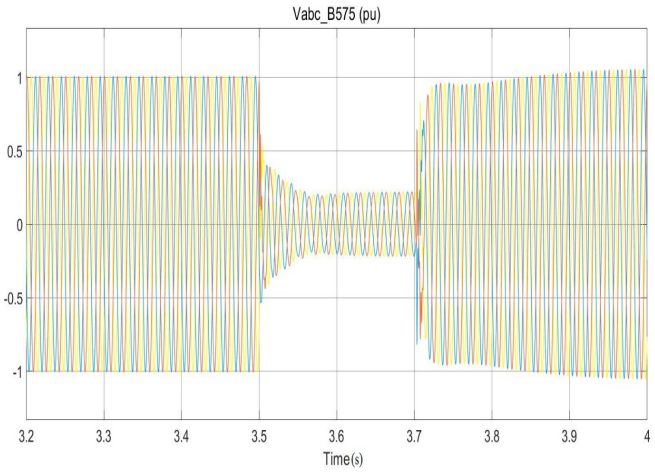

Fig. 7. Stator power winding voltage during symmetrical fault.

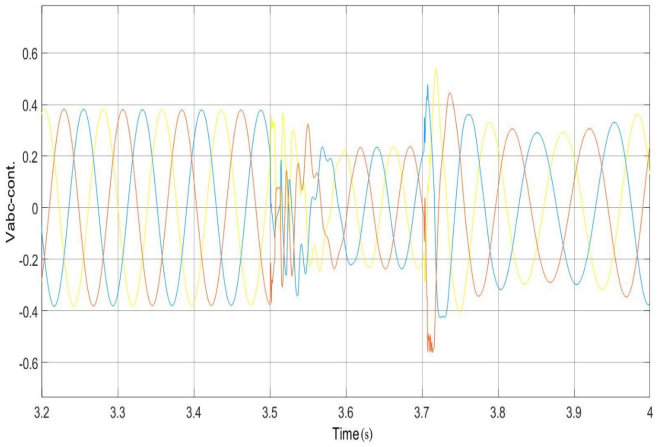

Fig. 8. Stator control winding voltage during symmetrical fault.

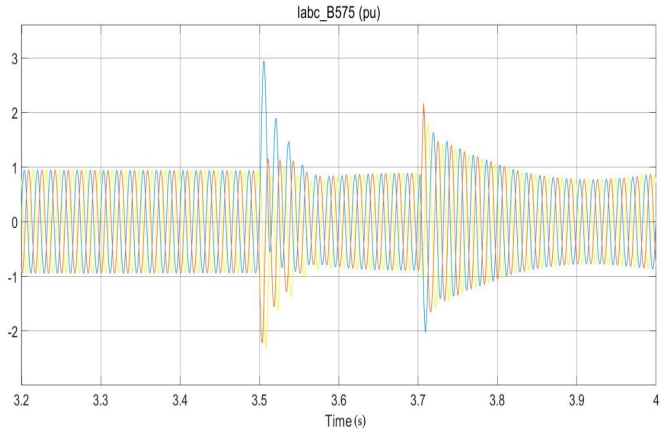

Fig. 9. Stator power winding current during symmetrical fault.

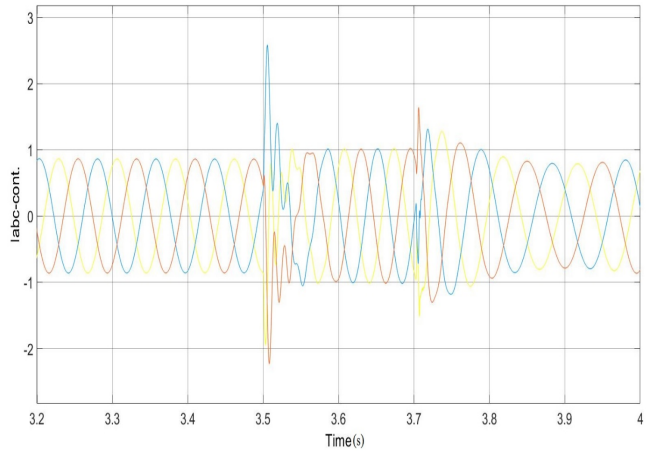

Fig. 10. Stator control winding current during symmetrical fault.

According to Figure 11, the DC link voltage has a slight fluctuation at the beginning of the fault, which even reaches up to 1250 volts; but it quickly returns to the reference value after a while. Figure 12 shows the rotor speed value in the BDFIG during the 100% voltage drop in the grid. During the fault occurrence, the speed has an overshoot up to 1.28 pu. Given that the generator type is a doubly-fed induction one with permissible speed variations up to ± 30%, thus, the studied speed can be controlled during the event of the fault.

B. Performance of The Proposed Structure During Asymmetrical Voltage Drop

An asymmetrical fault has been applied to the examined simulated structure between 3.5 and 3.7 seconds in the grid to evaluate the performance of the proposed structure when an asymmetrical fault occurs in the grid. According to Fig. 13 the power winding current value fluctuates around 1.4 pu during the occurrence of the asymmetrical voltage drop and the amount of its inrush currents has been significantly reduced. As shown in the Figure 14, the values of the control winding current are controlled up to about 1.2 pu during the occurrence of the asymmetrical drop. Figures 15 and 16 show the DC link voltage value in the average model converter and the rotor speed value, respectively. As shown in the figures, when an asymmetrical fault occurs in the grid, the mentioned values fluctuate around their reference value with acceptable values.

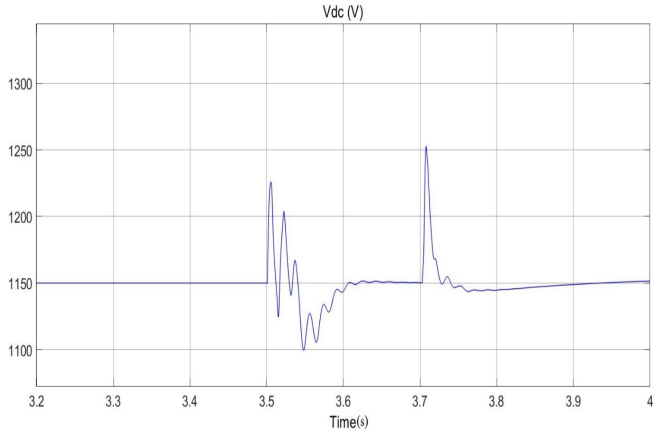

Fig. 11. DC link voltage during symmetrical fault.

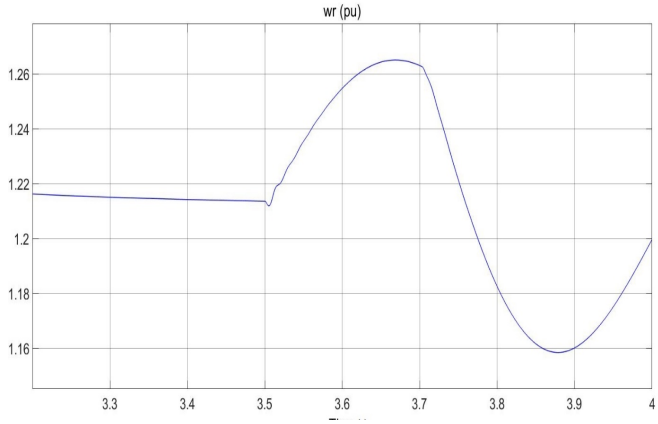

Fig. 12. Rotor speed during symmetrical fault.

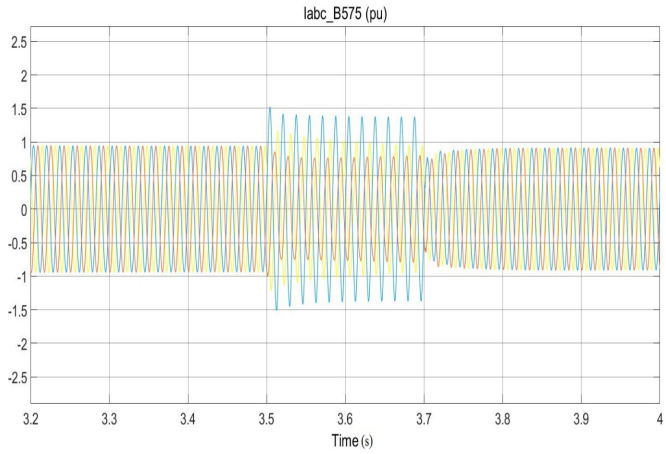

Fig. 13. Stator power winding current during asymmetrical fault.

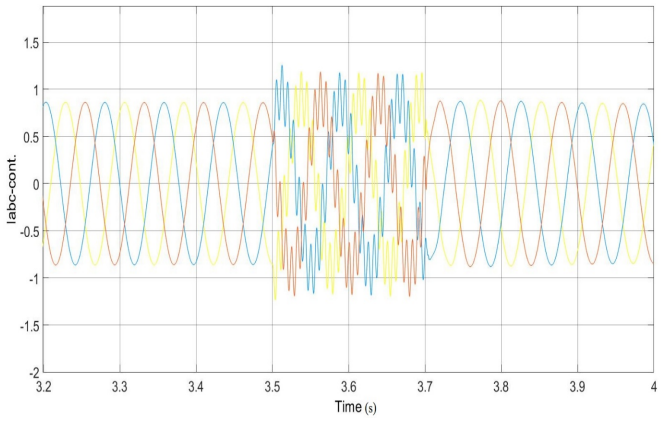

Fig. 14. Stator control winding current during asymmetrical fault.

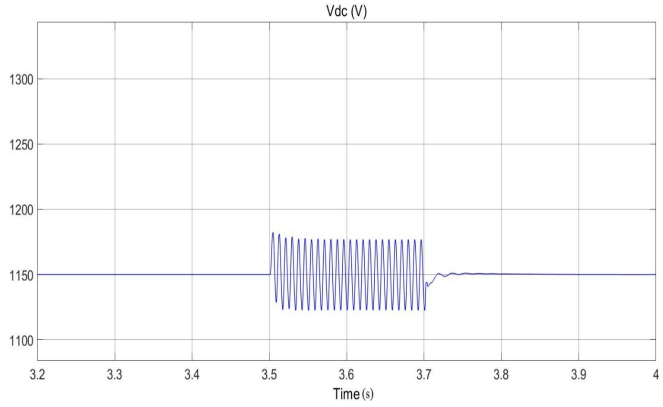

Fig. 15. DC link voltage during asymmetrical fault.

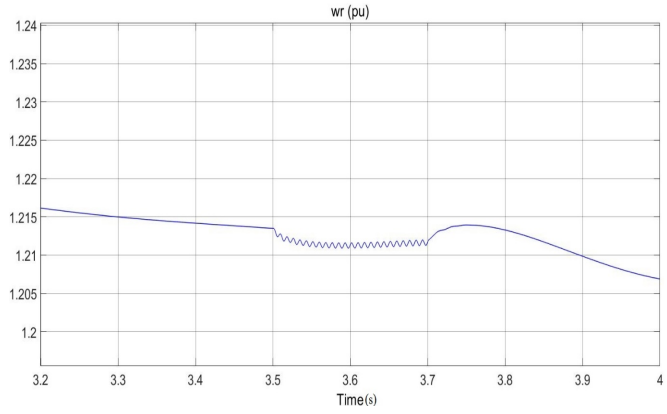

Fig. 16. Rotor speed during asymmetrical fault.

VI. CONCLUSION

In this paper, PI based controlling models have been used without using additional hardware such as crowbar for grid anomalous conditions which is based on the BDFIG average model. The examined structure first describes the model of a BDFIG in the dq two-axis frame, which DC link voltage is controlled and simulated in normal grid operating conditions without the use of a cross-compensator. In the occurrence of faults, huge excessive transient currents are generated in the generator stator windings, which damage the grid-side converters and the generator. Three control systems are provided for the grid-side converter, stator control winding side converter, and the wind turbine to prevent this and improve the LVRT capability during the occurrence of a fault. A closed-loop control system is used in the grid side converter to control the DC link voltage of the converter. The control system of the stator winding side converter itself consists of three control systems, which help improve the LVRT in the fault conditions. Finally, the proposed control model is used to control the wind turbines step angle. The occurrence of symmetrical and asymmetrical voltage drops in the power grid also has a controllable performance. During voltage drop caused by asymmetrical faults, we saw some fluctuations in the DC link voltage of the average model converter as well as in the electrical torque during the error time, resulted in partial improvement of the grid. During the occurrence of voltage drops due to symmetrical faults, the proposed structure is fully controlled and improved. Simulation results confirm the outcome.

REFERENCES

[1] K. H. Kim, Y. C. Jeung, D. C. Lee, and H. G. Kim, "LVRT scheme of PMSG wind power systems based on feedback linearization," *IEEE Trans. Power Electron.*, vol. 27, no. 5, pp. 2376–2384, 2012.

[2] T. Long, S. Shao, P. Malliband, E. Abdi, and R. a. McMahon, "Crowbarless fault ride-through of the brushless doubly fed induction generator in a wind turbine under symmetricalal voltage dips," *IEEE Trans. Ind. Electron.*, vol. 60, no. 7, pp. 2833–2841, 2013.

[3] S.Shiyi, E.Abdi, and R.McMahon, "Dynamic analysis of the brushless doubly-fed induction generator during symmetricalal three-phase voltage dips," *Power Electronics and Drive Systems, PEDS. International Conference on*, vol. 15, no. 4, pp. 464-469, 2009.

[4] S. Tohidi, H. Oraee, M. R. Zolghadri, S. Shao, and P. Tavner, "Analysis and enhancement of low-voltage ride-through capability of brushless doubly fed induction generator," *IEEE Trans. Ind. Electron.*, vol. 60, no. 3, pp. 1146–1155, 2013.

[5] T. Coso, E. Battaiotto, and R. Mantz. "Active and reactive power control capability in wind generation based on BDFIG machine," In *Innovative Smart Grid Technologies Latin America, IEEE PES*, vol. 7, no. 12, pp. 546-551, 2015.

[6] A. R. W. Broadway and L. Burbridge, "Self-cascade machine: A lowspeed motor or high frequency brushless alternator," *Proc. Inst. Elect. Eng.*, vol. 117, no. 7, pp. 1529–1535, 1974.

[7] R. A. McMahon, P. C. Roberts, X. Wang, and P. J. Tavner, "Performance of BDFM as generator and motor," *Proc. Inst. Elect. Eng.—Elect. Power Appl.*, vol. 153, no. 2, pp. 289–299, Mar. 2006.

[8] J. Poza, E. Oyarbide, and D. Roye, "New vector control algorithm for brushless doubly-fed machines," in *Proc. 28th Annu. IEEE IECON*, vol. 2, pp. 1138–1143, Nov. 2002.

[9] J. Poza, E. Oyarbide, D. Roye, and M. Rodriguez, "Unified reference frame dq model of the brushless doubly fed machine," *Proc. Inst. Elect. Eng.—Elect. Power Appl.*, vol. 153, no. 5, pp. 726–734, Sep. 2006.

[10] J. Lopez, P. Sanchis, X. Roboam, and L. Marroyo, "Dynamic behavior of the doubly fed induction generator during three-phase voltage dips," *IEEE Trans. Energy Convers.*, vol. 22, no. 3, pp. 709–717, Sep. 2007.